RAKE FINGER PLACEMENT FOR CDMA DOWNLINK EQUALIZATION

Haichang Sui, Elias Masry and Bhaskar D. Rao

Department of Electrical and Computer Engineering
University of California, San Diego
Email: {hsui,emasry,brao}@ucsd.edu

ABSTRACT

We consider the problem of interference suppression in multipath DS-CDMA downlink using a general RAKE receiver structure with M fingers and arbitrary finger delays. Utilizing asymptotically optimal sampling design theory, a new design approach that optimizes the receiver performance over the finger delays is proposed. It provides a set of delays which are asymptotically optimal for large M, and sheds light on the behavior of various finger placements' performance, as the number of fingers increases, and on the effect of the smoothness of the underlying chip pulse. Numerical results show that for certain Rayleigh fading channels and several chip pulses, the proposed finger placement is superior to the chip periodically-spaced finger placement.

1. INTRODUCTION

In DS-CDMA downlink systems, each user is assigned an orthogonal code. However, the orthogonality is lost due to the multipath channel. Among the various proposed techniques for interference suppression, linear processing is practical for mobile stations because of its low complexity. In the literature, "chip-level" algorithms have been developed, which performs interference suppression and despreading separately [1]-[3]. These receivers equivalently estimate the transmitted chip and try to restore the orthogonality between users by equalizing the downlink channel. Most previous studies assume a tapped-delay-line equalizer (TDLE) structure, with tap spacing equal to one or a fraction of the chip period. However, for linear estimation, this choice may not be optimal and a large number of taps would be necessary when the multipath span is much larger than the chip period. In [4], a general receiver model for linear chip-level interference suppression is proposed, of which the TDLE is a special case. It has a similar structure as the RAKE receiver, except the number of fingers and delay at each finger can be arbitrary. Two numerically-based suboptimal finger placement schemes are also presented in [4].

THIS RESEARCH WAS SUPPORTED BY CORE GRANT NO. 02-10109 SPONSORED BY ERICSSON.

In this paper, we employ the same general model as in [4] and propose an asymptotically optimal finger placement design. The approach is developed by establishing a relationship between optimal sampling design and optimal finger placement, and then employing results from asymptotical optimal sampling design [5]. The resulting set of delays is asymptotically optimal in the number of fingers for a wide class of the so-called "regular" finger placement schemes, including the uniformly spaced finger placement. Furthermore, in contrast to past work, this approach is analytical and shed lights on the behavior of various regular finger placements' performance as the number of fingers increases. In particular, it provides insight into the effect of the smoothness of underlying chip pulse on performance.

The rest of the paper is organized as follows. The system model is introduced in Section 2. In Section 3, we present the proposed finger placement design in detail. Numerical results are presented in Section 4.

2. SYSTEM MODEL

We consider a single-cell, downlink, DS-CDMA system with Q users and spreading gain N. The mth symbol transmitted by user k is denoted by $x_k[n]$. We assume the symbols are i.i.d. r.v.'s with zero mean and unit power. The spreading code for $x_k[n]$ is $[c_{n,k}[0], \ldots, c_{n,k}[N-1]]$, where $c_{n,k}[i] = w_k[i]\, s_n[i]$ for $i = 0, \ldots, N-1$. The code $[w_k[0], \ldots, w_k[N-1]]$ is orthogonal for different k and we assume it has unit norm. We also assume $s_m[n]$, the scrambling code, is QPSK modulated i.i.d. r.v., whose real and imaginary part independently take value from $\{\pm 1/\sqrt{2}\}$ with equal probability. Thus, the nth chip in the transmitted chip sequence is

$$e[n] = \sum_{k=1}^{Q} \sqrt{P_k} x_k[\lfloor n/N \rfloor]\, c_{\lfloor n/N \rfloor, k}[n \bmod N]$$

where P_k is the transmit power of user k. After chip-pulse-shaping, the continuous-time transmit signal is $e(t) = \sum_{n=-\infty}^{\infty} e[n]\, p(t - nT_c)$ where $1/T_c$ is the chip rate and $p(t)$ is the chip waveform. We assume $\int_{-\infty}^{\infty} |p(t)|^2\, dt = 1$. The signal received after propagating through a channel

with L paths, with gain α_l and delay τ_l on path l, is

$$r(t) = \sum_{l=1}^{L} \alpha_l e(t-\tau_l) + n_w(t) \quad (1)$$

where $n_w(t)$ is zero-mean complex white Gaussian noise process satisfying $E\{n_w(t+\tau) n_w^*(t)\} = N_0\delta(\tau)$.

The receiver is shown in Fig.1. The received signal $r(t)$ is passed through a chip matched-filter (MF) with impulse response $p^*(-t)$. Defining $R_p(t) \triangleq \int_{-\infty}^{\infty} p(u) p^*(u-t)\, dt$ and $q(t) \triangleq \sum_{l=1}^{L} \alpha_l R_p(t-\tau_l)$, it is easy to see that the output signal of chip MF is

$$v(t) = \sum_{n=-\infty}^{\infty} e[n]\, q(t-nT_c) + n_c(t) \quad (2)$$

where $n_c(t)$ is the filtered additive noise. We assume the receiver has M fingers wih finger location defined by $\mathbf{t} \triangleq [t_{1,M}, \ldots, t_{M,M}]^T$ with $t_{i,M} \in [a,b]$. Hence for estimating the chip $e[n]$, $v(t)$ is sampled to form $\mathbf{d}_n \triangleq [v(t_{1,M}+nT_c), \ldots, v(t_{M,M}+nT_c)]^T$ and the estimate of $e[n]$ is given by $\widehat{e}[n] = \mathbf{g}^H \mathbf{d}_n$. The symbol estimate is obtained by despreading the estimated chips. Reference [6] studied the properties of the weight vector $\mathbf{g}$ that minimizes the chip-level MSE $E\left|e[n] - \mathbf{g}^H \mathbf{d}_n\right|^2$. It is shown there that the chip MMSE is given by

$$MMSE(\mathbf{t}) = \sigma_e^2 \left[1 + \mathbf{q}_0^H(\mathbf{t})\, \mathbf{R}_u^{-1} \mathbf{q}_0(\mathbf{t})\right]^{-1} \quad (3)$$

where $\mathbf{q}_n(\mathbf{t})$ is an $M \times 1$ vector whose ith element is $q(t_{i,M}+nT_c)$; σ_e^2 is the energy per chip and $\sigma_e^2 = E|e[n]|^2 = \frac{1}{N}\sum_{k=1}^{Q} P_k$; $\mathbf{R}_u$ is the $M \times M$ matrix,

$$\mathbf{R}_u = \sum_{j \neq 0} \mathbf{q}_j(\mathbf{t})\, \mathbf{q}_j^H(\mathbf{t}) + \frac{N_0}{\sigma_e^2} \mathbf{R}_p(\mathbf{t}) \quad (4)$$

where the $M \times M$ matrix $\mathbf{R}_p(\mathbf{t})$ has $R_p(t_{i,M} - t_{j,M})$ as its i-jth element. This choice of $\mathbf{g}$ is also shown in [6] to maximize the SINR of the kth user's symbol estimates, $SINR_k$. In particular, $SINR_k(\mathbf{t}) = P_k/MMSE(\mathbf{t}) - P_k/\sigma_e^2$. Furthermore, if we assume that the interference plus noise term is approximately Gaussian, then the bit error probability of user k is $P_{e,k} = Q(\sqrt{(2\beta SINR_k)})$ where $\beta = 1$ for BPSK and $\beta = 1/2$ for QPSK modulated symbols [6].

3. ASYMPTOTICALLY OPTIMAL FINGER PLACEMENT

The problem of finger placement corresponds to choosing $\mathbf{t}$. We observe that the $\mathbf{t}$ minimizing the $MMSE(\mathbf{t})$ in (3) also maximizes $SINR_k$. However, $MMSE(\mathbf{t})$ depends on $\mathbf{t}$ in a nonlinear way, so exact optimization is not analytically tractable. Furthermore, $MMSE(\mathbf{t})$ is not a convex function of $\mathbf{t}$. We have observed in simulation that it has many local minima and the direct application of numerical optimization does not give satisfactory results.

In the following subsections, we first review the sampling design theory originally presented in [5] and extended by us to complex-valued random processes. Then we apply it to our problem and derive the set of finger delays that are asymptotically optimal in M.

3.1. Review of the sampling design theory

The sampling design theory addresses the problem of estimating a stochastic integral, $I = \int_a^b \phi^*(t) X(t) dt$ by a discrete sum $I_n \triangleq \sum_{i=0}^{n} c_{i,n}^* X(t_{i,n})$, where $X(t)$ is a second-order random process over $[a,b]$ with zero mean and covariance function $R(t,s) = E[X(t)X^*(s)]$. The quality of the estimator I_n is measured by $E|I - I_n|^2$. Denote by $T_n = \{t_{i,n}\}_{i=0}^n$ the set of sampling points. Once T_n is determined, the optimal weights $\{c_{i,n}\}_{i=0}^n$ are easy to derive by solving a set of Wiener-Hopf linear equations. We consider "regular" sampling designs generated by some positive continuous function $h(t)$ on $[a,b]$ via

$$\int_a^{t_{i,n}} h(t)dt = i/n \quad \text{for} \quad i = 1, \ldots, n \quad (5)$$

Note that choosing $h(t) = 1/(b-a)$ leads to uniform sampling, and the problem of optimal sampling corresponds to choosing an appropriate $h(t)$. We denote by $T_n(h)$ the set of n points specified by (5) and $I_n(h)$ to be the corresponding discrete sum. Under some regularity conditions, we have the following result [6]:

$$\lim_{n\to\infty} n^{2K+2} E|I - I_n(h)|^2 = \frac{|B_{2K+2}|}{(2K+2)!} \int_a^b \frac{|\phi(t)|^2\, Re[\alpha_K(t)]}{h^{2K+2}(t)} dt$$

where K is the exact quadratic-mean differentiability of $X(t)$, B_n is the Bernoulli number, and $\alpha_K(t) = R^{(K,K+1)}(t,t-) - R^{(K,K+1)}(t,t+)$. More technical details on the sampling design theory can be found in [6].

3.2. Applying the sampling design theory

The above result gives the mean-square-error of approximating a stochastic integral by a discrete sum. We now relate this approximation to our chip estimation problem. Consider the optimum continuous-time estimate of $e[0]$ by filtering $\{v(t), a \le t \le b\}$, that is, $\widehat{e}_{opt} \triangleq \int_a^b v(t)\, g_{opt}^*(t)\, dt$ where $g_{opt}(t)$ is the solution of the integral equation

$$\int_a^b R_v(t,u)\, g_{opt}(u)\, du = \sigma_e^2 q(t) \quad \text{for } t \in [a,b] \quad (6)$$

and $R_v(t,u) = E[v(t)\, v^*(u)]$. For any discrete estimate of the form $\widehat{e}_M = \sum_{i=1}^{M} g_{i,M}^* v(t_{i,M})$, we have

$$E|e[0] - \widehat{e}_M|^2 = MSE_{opt} + E|\widehat{e}_{opt} - \widehat{e}_M|^2 \quad (7)$$

where $MSE_{opt} \triangleq E\left|e\left[0\right]-\widehat{e}_{c,opt}\right|^2$. We see MSE_{opt} does not depend on either $\{g_{i,M}\}_{i=1}^{M}$ or $\{t_{i,M}\}_{i=1}^{M}$, and the second term in (7) is analogous to $E\left|I-I_n(h)\right|^2$. By applying the results in the previous subsection, we have

$$\begin{aligned} C\left(h\right) &\triangleq \lim_{M\to\infty} M^{2K+2}E\left|\widehat{e}_{c,opt}-\widehat{e}_M\right|^2 \\ &= \frac{\left|B_{2K+2}\right|}{(2K+2)!}\int_a^b \frac{\left|g_{opt}\left(t\right)\right|^2 \mathrm{Re}\left[\alpha_K\left(t\right)\right]}{h^{2K+2}\left(t\right)}dt \end{aligned}$$

for any set of finger delays $\{t_{i,M}\}_{i=1}^{M}$ generated by the design density $h(u)$. Consequently, for a sequence of regular sampling scheme $\{T_M\left(h\right)\}_M$ associated with $h\left(t\right)$, the chip estimation MSE satisfies

$$\lim_{M\to\infty} E\left|e\left[0\right]-\widehat{e}_M\right|^2 = MSE_{opt}$$

and the fractional MSE defined by $f_e\left(M,h\right) \triangleq \frac{E\left|\widehat{e}_{c,opt}-\widehat{e}_M\right|^2}{MSE_{opt}}$ satisfies,

$$\lim_{M\to\infty} M^{2K+2} f_e\left(M,h\right) = C'\left(h\right) \triangleq C(h)/MSE_{opt} \quad (8)$$

3.3. Implications

The result of the previous subsection is quite general in the sense that it holds for any "regular" finger placement scheme, including uniform and the asymptotically optimal design to be introduced later. The theory tells us that for any regular finger placement, the fractional MSE behaves like $C'(h)/M^{2K+2}$ for large M. The exponent of M depends on the order of quadratic-mean differentiability of $v\left(t\right)$. This is equivalent to the degree of differentiability of the covariance function

$$R_v\left(t,u\right) = \sigma_e^2 \sum_{n=-\infty}^{\infty} q\left(t-nT_c\right)q^*\left(u-nT_c\right) + N_0 R_p\left(t-u\right)$$

where $t,u \in [a,b]$. It is seen that the latter depends on the degree of differentiability of $R_p(\tau)$ which in turn depends on the smoothness of the chip pulse $p(t)$. Thus, the smoother $p(t)$ is, the faster is the rate of convergence of the chip mean-square estimation error. For example, when rectangular pulse is used, it is shown in [6] that $K=0$ and $\alpha_0(t) = 2N_0/T_c$ almost everywhere on $[a,b]$. If we convolve the rectangular pulse with itself, we get a triangular chip pulse for which $v(t)$ has exactly one quadratic-mean derivative, i.e., $K=1$. In this case $\alpha_1(t) = 72N_0/T_c^3$. More details can be found in [6].

Of all possible choices of $h(t)$, $h_u(t) = 1/(b-a)$ corresponds to the scenario that $t_{1,M},\ldots,t_{M,M}$ are equally spaced for any M. However, $h_u(t)$ is not optimal in terms of minimizing the asymptotic constant $C'(h)$ in general. The $h_{opt}\left(t\right)$ that minimizes $C'\left(h\right)$ is given by

$$h_{opt}(t) = \frac{1}{A}\left[\left|g_{opt}\left(t\right)\right|^2 \mathrm{Re}\left[\alpha_K\left(t\right)\right]\right]^{1/(2K+3)} \quad (9)$$

where A is a scaling constant to ensure that $h_{opt}(t)$ integrates to one over the interval $[a,b]$. For this choice of $h(t)$

$$C'\left(h_{opt}\right) = \frac{\left\{\int_a^b \left[\left|g_{opt}\left(t\right)\right|^2 \mathrm{Re}\left[\alpha_K\left(t\right)\right]\right]^{1/(2K+3)} dt\right\}^{2K+3}}{\left|B_{2K+2}\right|^{-1} MSE_{opt}\left(2K+2\right)!}$$

4. NUMERICAL RESULTS

In this section, we study numerically the potential benefit from optimizing the finger delays. All results are based on a downlink consisting of $Q=24$ users with $P_k=1$ for all k's. The spreading gain N is 32 and the chip rate is 3.6864MHz. Symbols are QPSK modulated and have unit energy ($E_b = 1/2$). We compare the average BER of different schemes over two 3-ray Rayleigh channel models. For both channel models, the amplitudes of channel gains $\alpha_1,\alpha_2,\alpha_3$ are Rayleigh r.v.'s with average power 0,-3,-8dB. The phase of each ray is uniform r.v. in $[0,2\pi)$. and we always assume $\tau_1=0$ to account for receiver synchronism. τ_2 and τ_3 are uniformly distributed in $[T_c,3T_c]$ and $[4T_c,6T_c]$ for the first channel model and $[T_c,10T_c]$ and $[11T_c,20T_c]$ for the second channel model. We choose $[a,b]=[-12T_c,12T_c]$ for the first channel model and $[a,b]=[-30T_c,30T_c]$ for the second model. The rationale behind this choice can be found in [6]. We use $E_{ch1}\{\cdot\}$ and $E_{ch2}\{\cdot\}$ to indicate averaging over 400 independent channel realizations for the first and second channel model, respectively.

Fig.2(a)-(b) shows the behavior of $E_{ch1}[f_e(M,h)]$ versus M for rectangular ($K=0$) and triangular ($K=1$) chip pulse, respectively. Two regular sampling schemes are shown, which correspond to $h_u(t) = \frac{1}{b-a}$ and $h_{opt}(t)$ of (9), where $g_{opt}(t)$ is the numerical solution of (6). For each $h(t)$, the asymptotic curve $E_{ch1}[C'_h]/M^{2K+2}$ is also plotted. We can see $E_{ch1}[f_e(M,h)]$ indeed converges to the asymptotic curve for both $h_u(t)$ and $h_{opt}(t)$, as predicted by (8). We note that $f_e\left(M,h\right)$ may not be monotonically decreasing as M increases. We do observe that the $f_e\left(M,h\right)$ curve with $h_{opt}\left(t\right)$ has less variations than that with $h_u\left(t\right)$.

In Fig.3(a)-(b), $E_{ch1}(P_e)$ versus E_b/N_0 curves are shown for rectangular pulse and triangular pulse, respectively. Curves in each subplot correspond to the conventional RAKE with optimal combining, asymptotically optimal finger placement scheme with 25 fingers, optimal continuous-time filter, and TDLE with $t_i = -12T_c + (i-1)T_c$ for $i=1,\ldots,25$. We notice that the asymptotically optimal scheme outperforms TDLE significantly at the same number of fingers.

We also compare different schemes when the second channel model is used. Fig.4(a)-(b) shows the average bit-error-probability of different schemes for rectangular and triangular pulse, respectively. The TDLE scheme sets $t_i = -30T_c + (i-1)T_c$ for $i=1,\ldots,61$. In addition to the RAKE with optimal combining, optimal continuous-time

filter, TDLE, and asymptotically optimal scheme with 61 fingers, we also plot the performance of asymptotically optimal scheme with 34 fingers, which is seen to outperforms the TDLE with 61 fingers by using roughly half the number of fingers. This could be a important advantage in terms of implementation complexity.

The effect of the chip pulse on the system performance can be observed by comparing the subplots (a) and (b) in Fig.3 and Fig.4, respectively. It is seen that for a given signal-to-noise ratio E_b/N_0, the BER for a triangular pulse is smaller than that of a rectangular pulse. This behavior makes sense and can be easily understood by examining equation (7). The second term is the integral approximation error which converges to zero faster for the triangular pulse because it is smoother than the rectangular pulse. Since the triangular and rectangular pulse have the same width, the first term in (7), which is the mean squared continuous-data estimation error, is smaller for a triangular pulse by virtue of the larger effective bandwidth it occupies.

5. REFERENCES

[1] I. Ghauri and D.T.M. Slock, "Linear receivers for the DS-CDMA downlink exploiting orthogonality of spreading sequences", *Proc. of 32th Asil. Conf.*, pp.650-654, Nov. 1998.

[2] G. Bottomley, T. Ottosson and Y.-P. Wang, "A generalized RAKE receiver for interference suppression", *IEEE J. on Selected Areas in Comm.*, pp.1536-1545, Aug. 2000.

[3] T. Krauss, W. Hillery and M. Zoltowski, "Downlink specific linear equalization for frequency selective CDMA cellular systems", *J. of VLSI Sig. Proc.*, 2002.

[4] H. Sui, E. Masry, B. D. Rao and Y. C. Yoon, "CDMA downlink chip-level MMSE equalization with finger placement", *Proc. of IEEE 37th Asilomar Conf.*, 2003.

[5] K. Benhenni and S. Cambanis, "Sampling design for estimating integrals of stochastic processes", *The Annals of Statistics*, vol.37, No.1, pp.66-89, Feb. 1966.

[6] H. Sui, E. Masry and B. D. Rao, "Chip-level DS-CDMA downlink interference suppression with optimized finger placement" *submitted to the IEEE Trans. Signal Processing.*

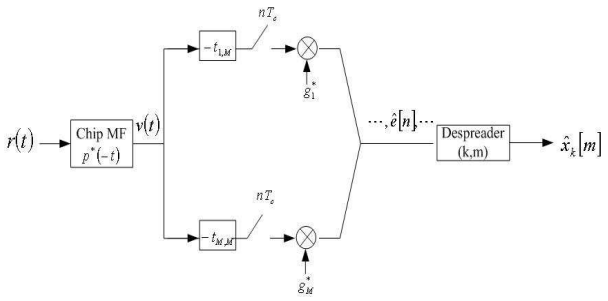

Fig. 1. Receiver structure

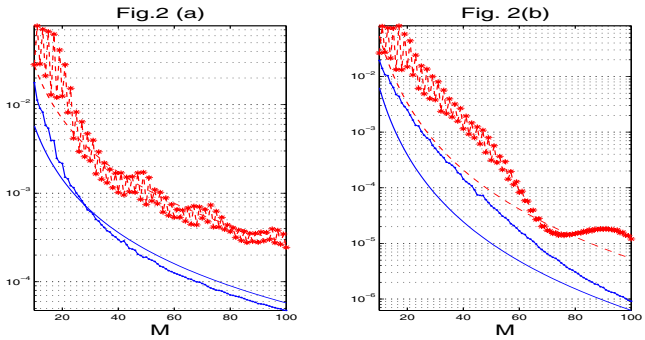

Fig. 2. $E_{ch1}[f_e(M,h)]$ and $E_{ch1}[C'(h)]/M^{2K+2}$ versus M: (a) rectangular pulse; (b) triangular pulse. (dashed with star: $E_{ch1}[f_e(M,h_u)]$; dashed: $E_{ch1}[C'(h_u)]/M^{2K+2}$; solid with dot: $E_{ch1}[f_e(M,h_{opt})]$; solid: $E_{ch1}[C'(h_{opt})]/M^{2K+2}$)

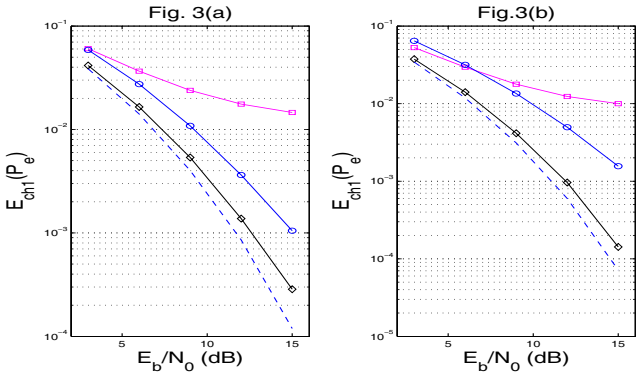

Fig. 3. $E_{ch1}(P_e)$ versus $E_b/N_0(dB)$ for the first channel model: (a) rectangular pulse; (b) triangular pulse. ('-□': RAKE with optimal combining, 3 fingers; '-○': T_c-spaced finger placement, 25 fingers; '-◊': Asymptotic optimal design, 25 fingers; '- -': Optimal continuous-time filter

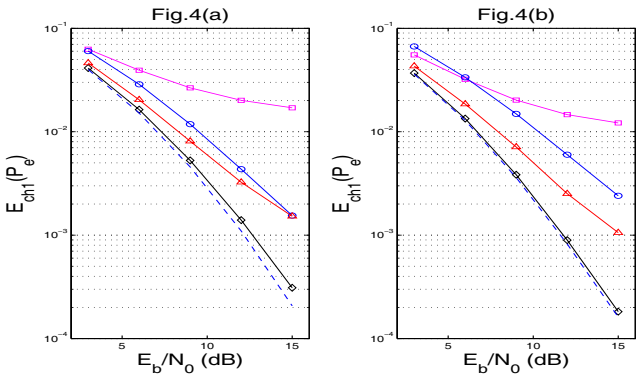

Fig. 4. $E_{ch2}(P_e)$ versus $E_b/N_0(dB)$ for the second channel model: (a) rectangular pulse; (b) triangular pulse. ('-□': RAKE with optimal combining, 3 fingers; '-○': T_c-spaced finger placement, 61 fingers; '-◊': Asymptotic optimal design, 61 fingers; '-△': Asymptotic optimal design, 34 fingers; '- -': Optimal continuous-time filter